Tumor and Stem Cell Biology

Cancer Research

Epigenetic Switch between *SOX2* and *SOX9* Regulates Cancer Cell Plasticity

Sheng-Chieh Lin[1], Yu-Ting Chou[1], Shih Sheng Jiang[2], Junn-Liang Chang[3,4], Chih-Hung Chung[5], Yu-Rung Kao[5], I-Shou Chang[2], and Cheng-Wen Wu[1,5,6,7,8]

Abstract

Cell differentiation within stem cell lineages can check proliferative potential, but nodal pathways that can limit tumor growth are obscure. Here, we report that lung cancer cell populations generate phenotypic and oncogenic plasticity via a switch between differentiation programs controlled by SOX2 and SOX9, thus altering proliferative and invasive capabilities. In lung cancer cells, SOX2 bound the *EPCAM* promoter to induce EpCAM–p21^{Cip1}–cyclin A2 signaling, encouraging cell proliferation as well as barrier properties. In contrast, SOX9 bound the *SLUG* promoter to induce SLUG-mediated cell invasion with a spindle-like phenotype. Pharmacologic inhibition of HDAC elevated a SOX9-positive cell population from SOX2-positive cells, whereas ectopic expression of SOX2 inhibited SOX9 with increased H3K9me2 levels on the *SOX9* promoter. In clinical specimens, the expression of SOX2 and SOX9 correlated negatively and positively with lung tumor grade, respectively. Our findings identify SOX2 and SOX9 as nodal epigenetic regulators in determining cancer cell plasticity and metastatic progression. *Cancer Res; 76(23); 7036–48. ©2016 AACR.*

Introduction

Epithelial-to-mesenchymal transition (EMT), defined by the loss of epithelial characteristics and acquisition of a mesenchymal phenotype, has significant roles in both normal embryonic development and cancer invasion (1, 2). Nonetheless, the reverse process [mesenchymal-to-epithelial transition (MET)] has been indicated to be essential for cancer progression (3–5). Cancer plasticity, a functional and phenotypic switch between mesenchymal-like and epithelial-like states in tumors, which correlate with invasion and proliferation, respectively, has been suggested to generate heterogeneity and control tumor progression (6, 7). Signaling networks orchestrated by master transcription factors determine stem cell fate and cancer cell identity (8, 9). However, the mechanism by which master transcriptional factors endow cells in tumors with diverse functions to generate cancer plasticity has been less well-studied.

SOX2, a master transcriptional factor involved in lung stem/progenitor cell functions, has been shown to promote tumor malignancy, thus linking stem/progenitor signaling with oncogenesis in lung cancer (10). SOX2 belongs to the SOX (Sry-related HMG Box) family of transcription factors and is essential for the maintenance of self-renewal and pluripotency in embryonic stem cells, as well as in adult tissue progenitor cells during lung development (11, 12). SOX2 signaling initiates the proliferation of lung stem/progenitor cells that line the respiratory tract and are critical for tissue homeostasis and cell proliferation during injury repair (13, 14). In addition, *SOX2* expression has been detected in human breast and lung cancers (15, 16), and genomic *SOX2* amplification has been observed in lung tumors, particularly of the squamous cell carcinoma subtype (17). *SOX2* overexpression in the lung epithelium of adult mice induces lung tumor formation (18), thus indicating an oncogenic role for SOX2 in lung tumors. Although SOX2 promotes both proliferation and survival in lung cancer cells (10) and maintains the tumor-initiating and self-renewal features in squamous cell carcinomas of the skin (19), the role of SOX2 in cancer invasion and metastasis is less well-understood.

SOX9, another member of the SOX family, has been reported to activate Slug and thus induces EMT during avian neural crest development (20). SOX9 regulates lung branching morphogenesis and is highly expressed in a subgroup of lung adenocarcinomas (21, 22). In addition, SOX9 plays a critical role in chondrocyte differentiation, and cooperation between SOX9 and Slug has been shown to determine the mammary stem cell fate and encourage malignancy in breast cancer (23, 24).

Herein, we observed that *SOX2* is expressed in highly proliferative but minimally invasive lung cancer cells; in contrast, cells selected for invasiveness exhibited enriched *SOX9* expression but attenuated *SOX2* expression, leading to reduced cell proliferation and increased invasiveness. We further revealed that the switch between *SOX2* and *SOX9* expression is epigenetically controlled and allows cancer cells to exhibit plasticity characterized by distinct proliferative and invasive properties.

[1]Institute of Biotechnology, College of Life Science, National Tsing Hua University, Hsinchu, Taiwan. [2]National Institute of Cancer Research, National Health Research Institutes, Miaoli, Taiwan. [3]Department of Pathology and Laboratory Medicine, Taoyuan Armed Forces General Hospital, Taoyuan, Taiwan. [4]Department of Biomedical Engineering, Ming Chuan University, Taoyuan, Taiwan. [5]Institute of Biomedical Sciences, Academia Sinica, Taipei, Taiwan. [6]Institute of Biochemistry and Molecular Biology, National Yang-Ming University, Taipei, Taiwan. [7]Institute of Clinical Medicine, National Yang-Ming University, Taipei, Taiwan. [8]Institute of Microbiology and Immunology, National Yang-Ming University, Taipei, Taiwan.

Note: Supplementary data for this article are available at Cancer Research Online (http://cancerres.aacrjournals.org/).

Corresponding Authors: Cheng-Wen Wu, National Yang-Ming University, No. 155, Sec. 2, Linong Street, Taipei 11221, Taiwan. Phone: 886-2-2826-7919; Fax: 886-2-2823-6518; E-mail: cwwu@ym.edu.tw; and Yu-Ting Chou, National Tsing Hua University, No. 101, Sec. 2, Kuang-Fu Road, Hsinchu 30013, Taiwan. Phone: 886-3-574-2471; Fax: 886-3-571-5934; E-mail: ytchou@life.nthu.edu.tw

doi: 10.1158/0008-5472.CAN-15-3178

AACR

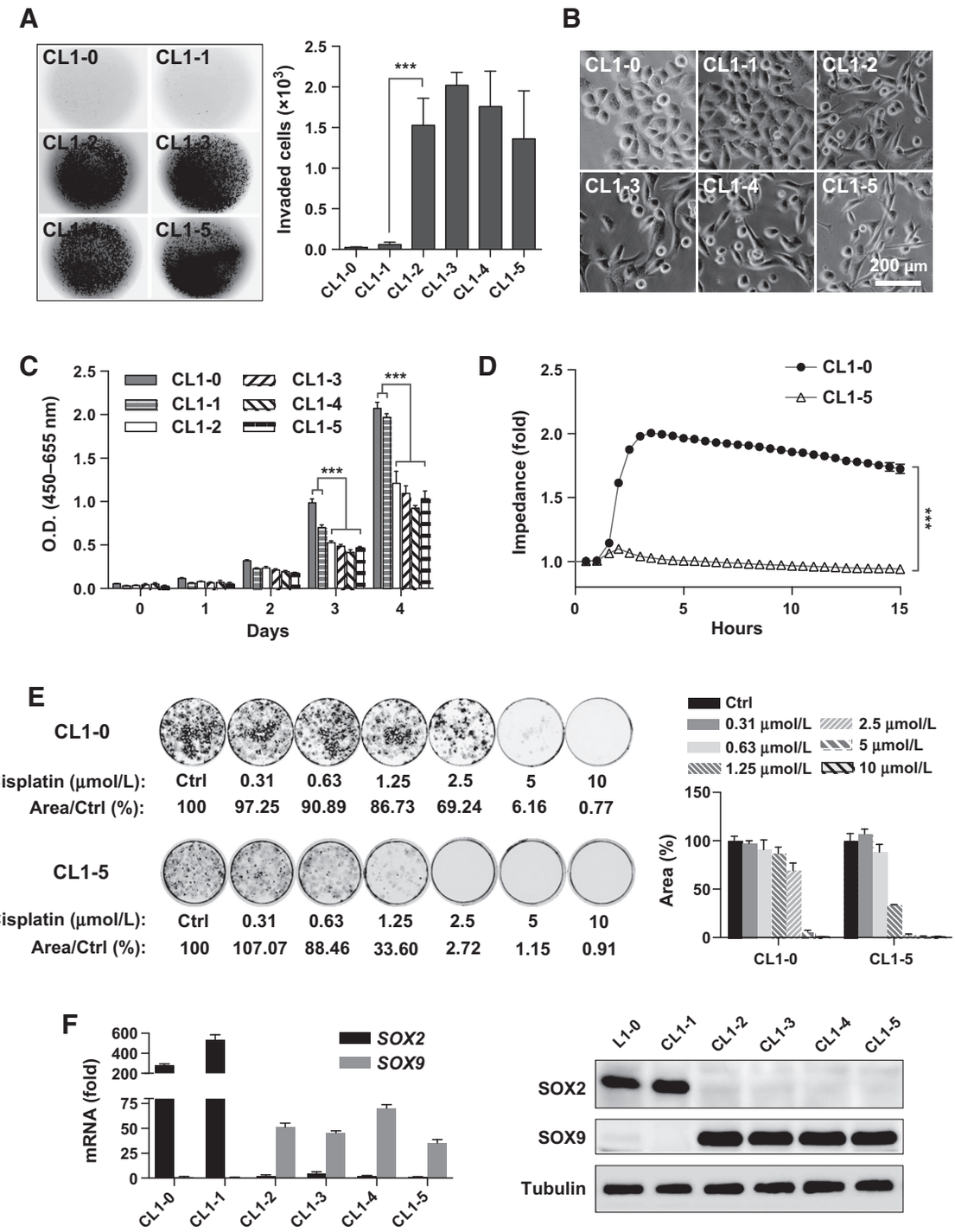

Figure 1.

Negative interplay between proliferation and invasion. **A,** *In vitro* invasion assay for determining the invasiveness of CL1-0 cells and its *in vitro* invasion selection derivatives (CL1-1–CL1-5). The invaded cells were stained with propidium iodide (left) and quantified (right). **B,** Phase-contrast images of CL1-0 and its derivatives. **C,** WST-1 cell proliferation analysis of CL1-0 and its derivatives. **D,** ECIS analysis in CL1-0 and CL1-5 cells for measuring barrier properties. *x*-axis, time (h); *y*-axis, normalized impedance (fold change). **E,** Clonogenic assay for comparing the cisplatin-mediated cytotoxic effect on CL1-0 cells with that on CL1-5 cells (left). Quantitative analysis of the data from the clonogenic assay (right). **F,** qPCR (left) and immunoblotting (right) for the expression of SOX2 and SOX9 in CL1-0 and its derivatives.

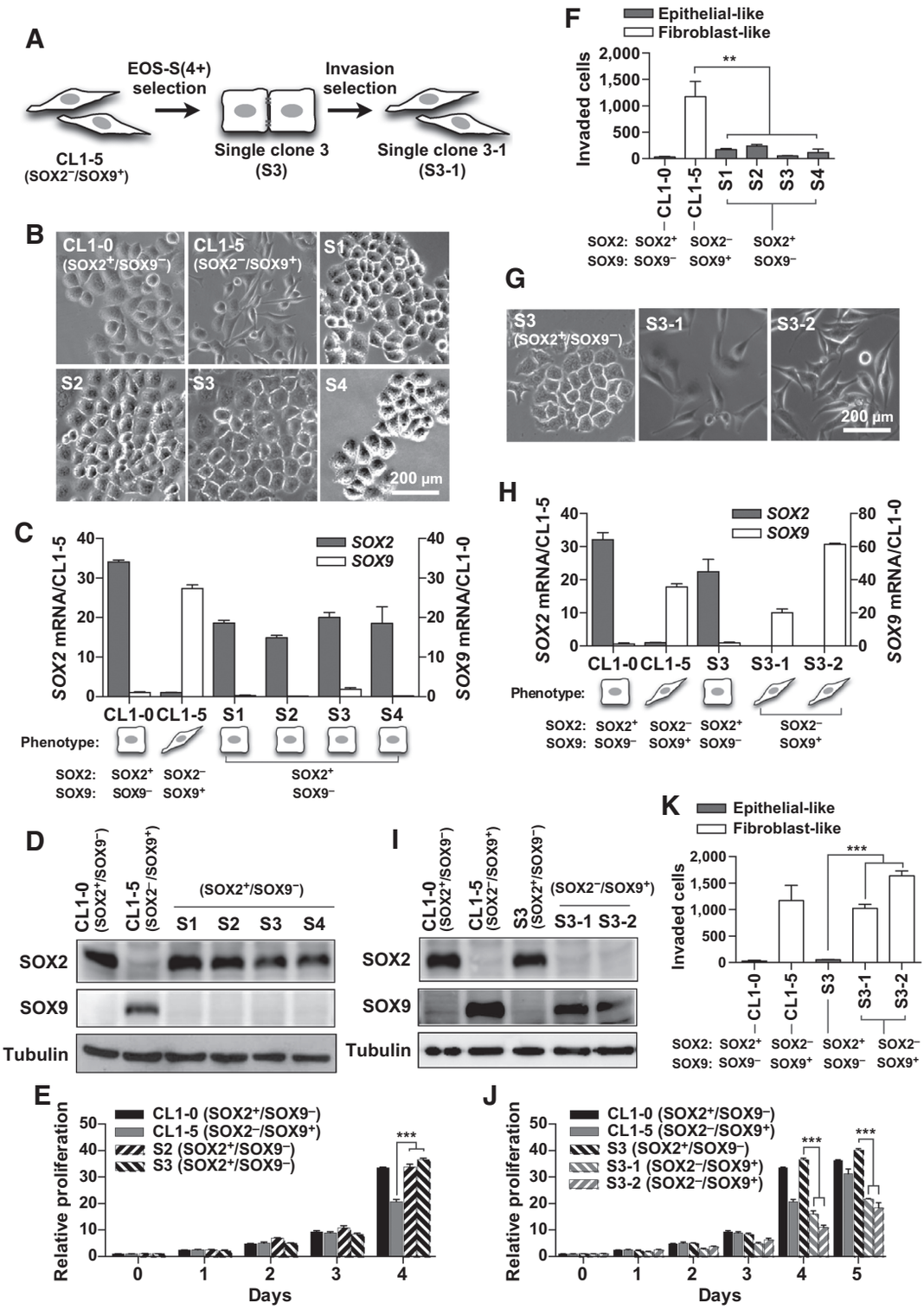

Figure 2.

Switching expression between *SOX2* and *SOX9* controls cancer cell plasticity. **A,** Schematic diagram for sequential selection of SOX2-positive and invasive lung cancer cells with EOS-S(4+) and invasion assays. CL1-5 (SOX2-negative) cells were infected with EOS-S(4+) lentiviral vectors, followed by puromycin selection to identify S1∼S4, 4 SOX2-positive clones. S3, a SOX2-positive clone, was further subjected to an invasion assay to obtain S3-1 and S3-2 invasive clones. **B,** Phase-contrast images of S1∼S4 as well as parental CL1-5 and CL1-0 cells. (*Continued on the following page.*)

Materials and Methods

Cell culture

CL1 series cells (CL1-0–CL1-5) were established in our laboratory as previously described (25) and further certified via STR-PCR DNA profiling in 2015. H1975 cells were kindly provided by Dr. Wun-Shaing W. Chang at the National Health Research Institutes, Taiwan, and further authenticated via *EGFR* sequencing analysis in 2015. All lung cancer cells were cultured in RPMI-1640 medium containing 4 mmol/L L-glutamine, 1 mmol/L sodium pyruvate, 10 mmol/L HEPES, and 10% FBS.

Plasmid construction and viral infection

Human *SOX9* or *EPCAM* cDNA were purchased from Thermo Scientific and subcloned into the pHR'-puro vector. pHR'-*SOX2* and pLKO.1-*SOX2* were described previously (10). shRNA clones of pLKO.1-*SOX9*, -*EPCAM*, or -*HDAC1* were obtained from the National RNAi Core Facility, Academia Sinica, Taiwan. The *SLUG* promoter region (−1,140 to +175 bp) was amplified from gDNA and subcloned into the pGL3-basic vector. Detailed information about the shRNA clones is provided in Supplementary Table S1. Lentiviral production and infection were performed as described previously (26).

Immunoblotting

Cells were harvested in RIPA lysis buffer supplemented with a protease inhibitor cocktail. The antibodies against specific proteins and the titers used in this study are listed in Supplementary Table S2.

Matrigel invasion assay

An *in vitro* invasion assay was performed using a FluroBlok 24-multiwell cell culture insert system (BD Biosciences); detailed procedures for the invasion assay are described in the Supplementary Information.

Electric cell–substrate impedance sensor analysis

The gold electrodes of electric cell–substrate impedance sensor (ECIS) culturewares (8W10E+ or 8W1E) were coated with a 10 mmol/L cysteine solution. A total of 1.5×10^5 cells in 200 μL of medium were inoculated into the well, and the barrier functions of cells were monitored under a current of 4,000 Hz for 18 hours, using an ECIS model 8Z device (Applied Biophysics).

Immunostaining

Detailed immunostaining procedures are described in the Supplementary Information.

Chromatin immunoprecipitation-qPCR

Chromatin immunoprecipitation (ChIP) was performed using a LowCell# ChIP kit (Diagenode) as previously described (26, 27). Detailed procedures and materials for the ChIP assay are described in the Supplementary Information and Supplementary Table S3, respectively.

Human lung cancer

A lung cDNA array comprising 40 lung tumor cDNAs and 8 normal tissue cDNAs was purchased from OriGene Technologies for quantitative real-time (Q)-PCR analysis. Human lung cancer tissue arrays (CC5 and CCA4) were obtained from SuperBioChips Laboratories for the immunohistochemical analysis.

Cell proliferation assay

A WST-1 cell proliferation assay was performed as previously described (10).

Animal experiments

Tumor growth assays were conducted as previously described (10, 26). Detailed procedures for the xenograft assays are described in the Supplementary Information.

Public domain data analysis

The public gene expression profiling datasets used in this study were analyzed as described previously (22). The sources of these gene expression profiling datasets are listed in Supplementary Table S4. The median *SOX2* and *SOX9* levels were used as cutoff points for the overall survival analysis.

Statistical analysis

Differences in the immunohistochemical staining of human lung cancer specimens were assessed using a Pearson correlation analysis. Associations among the various markers and levels were calculated using Spearman rho correlation coefficient. $P < 0.05$ was considered to indicate a significant difference. All statistical analyses were performed using SPSS software, version 16 (SPSS, Inc.).

Results

Negative interplay between cancer cell proliferation and invasion

We previously established a series of human lung adenocarcinoma cell lines with differing invasive abilities via serial selection in a Boyden chamber assay (lines CL1-0–CL1-5; ref. 25) and demonstrated strong expression of SOX2 in CL1-0 cells (10). To investigate the interplay of SOX2 with cancer cell invasion and proliferation, CL1-0 and its invasive derivatives were subjected to proliferation and invasion assays. Invasion analysis revealed that these cells could be categorized into 2 groups: low-invasive (CL1-0 and CL1-1) and high-invasive (CL1-2, CL1-3, CL1-4, and CL1-5) cells (Fig. 1A). In addition, these cells exhibited distinct morphologic phenotypes that were visible under a phase-contrast microscope. Low-invasive cells exhibited an epithelial adhesive phenotype, whereas the high-invasive cells displayed a spindle fibroblast-like morphology (Fig. 1B). A cell proliferation assay

(*Continued.*) **C,** qPCR for the expression of *SOX2* (left) and *SOX9* (right) in CL1-0, CL1-5, and S1∼S4. **D,** Immunoblotting for the expression of SOX2 and SOX9 in CL1-0, CL1-5, and S1∼S4. **E,** WST-1 assay for comparing the cell proliferation potential of S2 and S3 with that of parental CL1-5 and CL1-0 cells. **F,** *In vitro* invasion assay for comparing the invasive ability of S1∼S4 with that of parental CL1-5 and CL1-0 cells. **G,** Phase-contrast images of invasion-selected clones S3-1 and S3-2 as well as parental S3 clone. **H,** qPCR analysis to compare the mRNA expression of *SOX2* and *SOX9* in S3, S3-1, and S3-2 with that in CL1-0 and CL1-5. **I,** Immunoblotting analysis for comparing the expression of SOX2 and SOX9 in S3, S3-1, and S3-2 with that in CL1-0 and CL1-5 cells. **J,** WST-1 assay for comparing the cell proliferation potential of S3, S3-1, and S3-2 clones with that of CL1-0 and CL1-5 cells. **K,** Invasion assay for comparing invasive ability of S3, S3-1, and S3-2 with that of CL1-0 and CL1-5 cells.

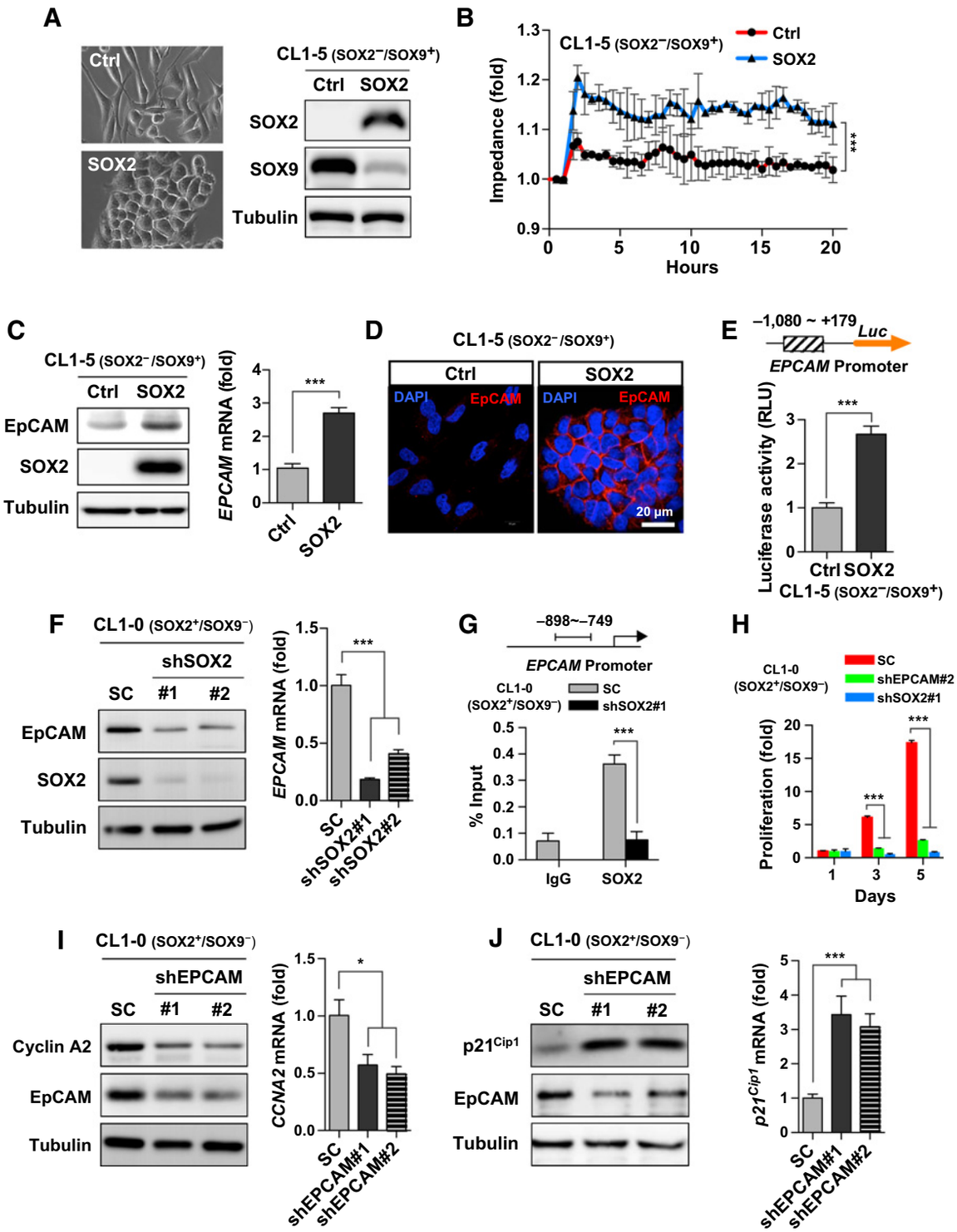

Figure 3.

SOX2 mediates EpCAM–p21^{Cip1}–cyclin A2 proliferative signaling. **A,** Phase-contrast images (left) and immunoblotting (right) in *SOX2*-overexpressing (SOX2) or control (Ctrl) CL1-5 cells. **B,** ECIS analysis for measuring barrier properties in CL1-5 cells infected with lentiviral vectors encoding *SOX2* cDNA (SOX2) or empty control vector (Ctrl). *x*-axis, time (h); *y*-axis, normalized impedance (fold change). **C,** Immunoblotting (left) and qPCR (right) analyses for measuring protein and mRNA levels of *EpCAM*, respectively, in CL1-5 cells infected with lentiviral vectors encoding *SOX2* cDNA (SOX2) or control vector (Ctrl). **D,** Immunofluorescent images of EpCAM (red) and DAPI (blue) in SOX2-overexpressing or control CL1-5 cells. Scale bar, 20 μm. (*Continued on the following page.*)

revealed that low-invasive CL1-0 and CL1-1 cells had a higher proliferation rate than did the high-invasive cells, indicating the presence of a negative correlation between cancer cell proliferation and invasion (Fig. 1C). An ECIS assay revealed a higher level of impedance in epithelial-like CL1-0 cells than in fibroblast-like CL1-5 cells (Fig. 1D). Moreover, we observed that CL1-0 cells were more resistant to cisplatin than were CL1-5 cells (Fig. 1E and Supplementary Fig. S1). A gene expression microarray analysis identified differing expression levels of *SOX2* and *SOX9* in the proliferative and invasive cells; these differences were further confirmed by qPCR and immunoblotting (Fig. 1F). These observations suggest different roles for SOX2 and SOX9 in the oncogenesis of lung cancer cells.

Switching between *SOX2* and *SOX9* expression modulates cancer cell plasticity

Because *SOX2* and *SOX9* are differentially expressed in proliferative and invasive lung cancer cells, we further examined whether mutual suppression between *SOX2* and *SOX9* would endow cells with proliferative and invasive abilities, thus generating cancer cell heterogeneity. To trace endogenous SOX2 signaling, we used an EOS-S(4+) reporter plasmid to isolate SOX2-positive clones from CL1-5 (SOX2-low) cells (Fig. 2A). The EOS-S (4+) reporter plasmid, which contains 4 repeats of the *SOX2* regulatory region 2 (SRR2), was originally used to screen endogenous SOX2-activated induced pluripotent stem (iPS) cells (28). After transducing CL1-5 cells with an EOS-S(4+) lentiviral plasmid, followed by single-clone isolation, we were able to identify 4 clones with an epithelial phenotype (S1, S2, S3, and S4; Fig. 2B). qPCR and immunoblotting revealed that *SOX2*, but not *SOX9*, was expressed in these CL1-5 descendants (Fig. 2C and D). These clones exhibited a higher proliferative potential but reduced invasive ability when compared with unaltered CL1-5 cells (Fig. 2E and F), suggesting that SOX2 inhibits invasion. To monitor the negative interplay between SOX2 signaling and invasion, S3, a SOX2-positive CL1-5 descendant, was subjected to invasion analysis (Fig. 2A). Transwell invasion screening identified two S3 descendant clones, S3-1 and S3-2, with a mesenchymal phenotype (Fig. 2G). Short tandem repeat (STR) analysis confirmed the genomic backgrounds of these established clones (Supplementary Fig. S2). qPCR and immunoblotting revealed that *SOX9*, but not *SOX2*, was expressed in S3-1 and S3-2 cells (Fig. 2H and I). These clones exhibited a lower proliferative potential but increased invasive ability relative to S3 parent cells (Fig. 2J and K). Similarly, SOX2-positive single clones were isolated from H1975 via the EOS-S(4+) reporter system (Supplementary Fig. S3A). These H1975 descendants exhibited increased SOX2 expression and decreased SOX9 expression and displayed an epithelial phenotype, increased cellular proliferation, and decreased invasive ability (Supplementary Fig. S3A–S3D). These data support the existence of a negative interplay between SOX2 and SOX9, which are respectively associated with cancer cell proliferation and invasion and determine the distinct phenotypes of lung cancer cells.

SOX2 regulates the EpCAM–p21^{Cip1}–cyclin A2 signaling axis, encouraging tumor cell proliferation

We further examined the role of SOX2 in the determination and maintenance of lung cancer cell epithelial morphology. Ectopic SOX2 expression shifted the fibroblast-like morphology of CL1-5 cells to an epithelial morphology with improved barrier function (Fig. 3A and B). Moreover, *SOX2* expression was associated with reduced *SOX9* expression (Fig. 3A and Supplementary Fig. S4). Because EpCAM mediates cell–cell adhesion and maintains stem/progenitor cell properties by regulating proliferation in solid tumors (29–32), we investigated the possible role of EpCAM in SOX2-induced oncogenesis. Immunoblotting and qPCR confirmed that the SOX2 expression led to elevated levels of *EPCAM* mRNA and protein (Fig. 3C). Immunofluorescent staining showed that SOX2 expression induced EpCAM expression in CL1-5 cells, thus encouraging cell–cell adhesion (Fig. 3D). Moreover, SOX2 knockdown attenuated the expression of EpCAM, indicating that SOX2 regulates EpCAM (Fig. 3F). Ectopic SOX2 expression led to enhanced *EPCAM* promoter reporter activity (Fig. 3E). To investigate the possible binding of SOX2 to the *EPCAM* promoter, SOX2-silenced and control CL1-0 cells were subjected to a ChIP analysis (Fig. 3G). SOX2 occupancy within the −898 to −749 bp region of the *EPCAM* promoter decreased upon SOX2 knockdown, indicating that SOX2 binds to the *EPCAM* promoter. To study the role of SOX2–EpCAM signaling in cancer cell proliferation, both EpCAM and SOX2 were silenced in CL1-0 cells, which were then used in a WST-1 cell proliferation assay. Knockdown of either EpCAM or SOX2 inhibited cell proliferation, supporting the idea that SOX2–EpCAM signaling regulates cell growth (Fig. 3H and Supplementary Fig. S5A and S5B). Because cyclin A2 and p21^{Cip1} positively and negatively regulate the cell cycle, respectively, and because the expressions of these proteins correlate with cancer malignancy (33, 34), we further tested the effect of EpCAM on cyclin A2 and p21^{Cip1} expression. EpCAM knockdown attenuated both the protein and mRNA levels of *CCNA2* (Fig. 3I). Furthermore, CCNA2 knockdown decreased the growth ability of CL1-0 cells (Supplementary Fig. S6). In contrast, EpCAM silencing increased both the protein and mRNA levels of *p21^{Cip1}* (Fig. 3J). These findings suggest that the EpCAM–p21^{Cip1}–cyclin A2 signaling axis is involved in SOX2-mediated cancer cell proliferation.

The SOX9–SLUG signaling axis controls tumor invasion

To evaluate the role of SOX9 in oncogenesis, we knocked down SOX9 in CL1-5 cells, which were then subjected to various *in vitro* functional analyses. SOX9 knockdown converted the fibroblast-like phenotype of CL1-5 cells to an epithelial morphology (Fig. 4A). Ectopic SOX9 expression in CL1-0 cells induced a mesenchymal phenotype, suggesting that SOX9 regulates cancer cell plasticity (Fig. 4A). ECIS analysis indicated that SOX9

(*Continued.*) **E,** *EPCAM* promoter reporter analysis in CL1-5 cells transfected with the pGL3-*EPCAM* promoter reporter plus or minus *SOX2* cDNA. **F,** Immunoblotting (left) and qPCR (right) analyses for measuring protein and mRNA levels of EpCAM, respectively, in CL1-0 cells infected with lentiviral vectors encoding shRNA against SOX2 (shSOX2) or scrambled control (SC). **G,** ChIP assay for detecting the occupancy of SOX2 at the −898 to −749 bp region of *EPCAM* promoter. SOX2 binding to *EPCAM* promoter was detected in CL1-0 cells infected with scrambled control or shSOX2 lentiviral vectors. Results are represented as mean ± SD. **H,** WST-1 cell proliferation analysis of CL1-0 cells infected with lentiviral vectors encoding shRNA against EpCAM (shEPCAM), SOX2 (shSOX2), or scrambled control. **I,** Immunoblotting (left) and qPCR (right) analyses for detecting protein and mRNA levels of *CCNA2*, respectively, in CL1-0 cells infected with lentiviral vectors encoding shEPCAM or a scrambled control. **J,** Immunoblotting (left) and qPCR (right) analyses for detecting protein and mRNA levels of *p21^{Cip1}* in CL1-0 cells infected with lentiviral vectors encoding shEPCAM or a scrambled control.

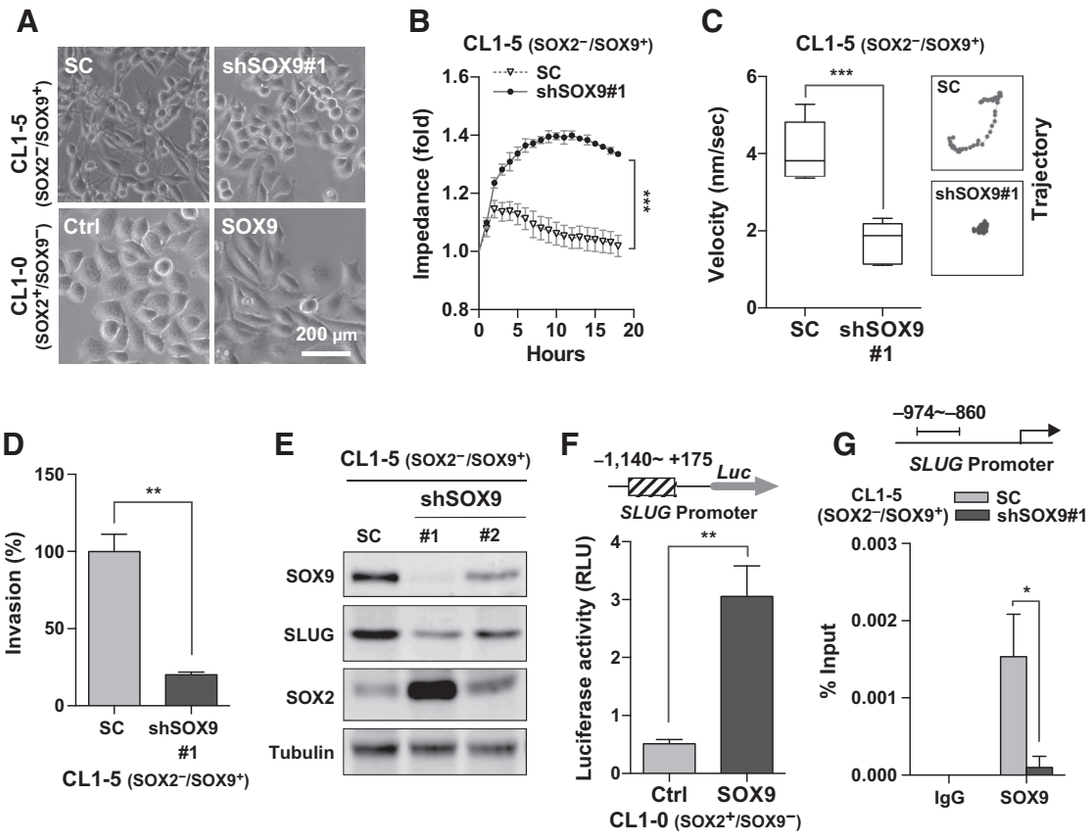

Figure 4.

SOX9 induces SLUG invasive signaling. **A,** Representative phase-contrast images of SOX9-silenced CL1-5 cells infected with shSOX9 (shSOX9#1) or scrambled control lentiviral vectors (top) or SOX9-overexpressing CL1-0 cells infected with *SOX9* cDNA or empty control lentiviral vectors (bottom). Scale bar, 200 μm. **B,** ECIS analysis for measuring barrier properties in CL1-5 cells infected with shSOX9 (shSOX9#1) or scrambled control (SC) lentiviral vectors. **C,** Cell tracking analysis for measuring the velocity (left) and trajectory (right) of CL1-5 cells infected with shSOX9 (shSOX9#1) or a scrambled control. The bars show the average of 10 single cells. **D,** Invasion assay of CL1-5 cells infected with shSOX9 (shSOX9#1) or scrambled control (SC) lentiviral vectors. **E,** Immunoblotting for comparing the expression of SOX9, SOX2, and SLUG in SOX9-silenced CL1-5 cells infected with a scrambled control or shSOX9 (shSOX9#1 or shSOX9#2) lentiviral vectors. shSOX9#1 and shSOX9#2 target different regions of SOX9 mRNA. **F,** *SLUG* promoter reporter analysis in CL1-5 cells transfected with the pGL3-*SLUG* promoter reporter plus or minus *SOX9* cDNA. **G,** ChIP assay for detecting the occupancy of SOX9 at the −974 to −860 bp region of the *SLUG* promoter in CL1-5 cells infected with a scrambled control or shSOX9 (shSOX9#1) lentiviral vectors.

knockdown increased the barrier properties of these cells (Fig. 4B). Furthermore, SOX9 silencing impaired the cell migration and invasiveness of CL1-5 tumor cells (Fig. 4C and D). A clonogenic analysis and WST-1 cell proliferation assay showed that SOX9 knockdown enhanced cell proliferation (Supplementary Fig. S5C and S5D). Immunoblotting revealed that SOX9 silencing led to increased levels of SOX2 but attenuated levels of SLUG, a key regulator of cancer plasticity and invasion (Fig. 4E). A luciferase promoter reporter analysis indicated that SOX9 expression led to *SLUG* promoter transactivation (−1,140 to +175 bp; Fig. 4F). A potential SOX9 binding motif was identified in the −974 bp to −860 bp region of the *SLUG* promoter. Using ChIP, we observed the attenuated occupancy of SOX9 on the −974 bp to −860 bp region of the *SLUG* promoter in SOX9-silenced cells, supporting the idea that SOX9 binds to the *SLUG* promoter (Fig. 4G). Therefore, our data indicate that SOX9 inhibits SOX2 expression but promotes SLUG expression, thereby attenuating barrier properties and promoting increased invasiveness in lung cancer cells.

SOX2 and SOX9 mediate tumor growth and invasion, respectively, in animal models

To evaluate the involvement of SOX2 in tumor growth, SOX2 was knocked down in CL1-0 cells; these cells were subsequently used in a subcutaneous xenograft assay conducted in immunodeficient mice. We found that whereas CL1-0 parent cells formed tumors in this animal model, this tumor-forming ability was inhibited in SOX2-silenced cells, suggesting that SOX2 regulates tumor cell growth *in vivo* (Fig. 5A). To evaluate the participation of SOX9 in tumor invasion *in vivo*, $SOX2^+/SOX9^-$ CL1-0 and $SOX2^-/SOX9^+$ CL1-5 cells were intravenously injected into nude mice. An *in vivo* imaging system (IVIS) analysis revealed a greater incidence of CL1-5 tumors than of CL1-0 tumors on day 14 after injection (Fig. 5B). To further study the role of SOX9 in cancer cell invasion *in vivo*, SOX9 was silenced in CL1-5 cells, which were then used for an intravenous xenograft analysis. IVIS analysis revealed that SOX9 knockdown attenuated the lung invasiveness of intravenously injected CL1-5 cells (Fig. 5C–F and Supplementary Fig. S7). These results suggest that SOX2 and SOX9 play distinct roles *in vivo*. We

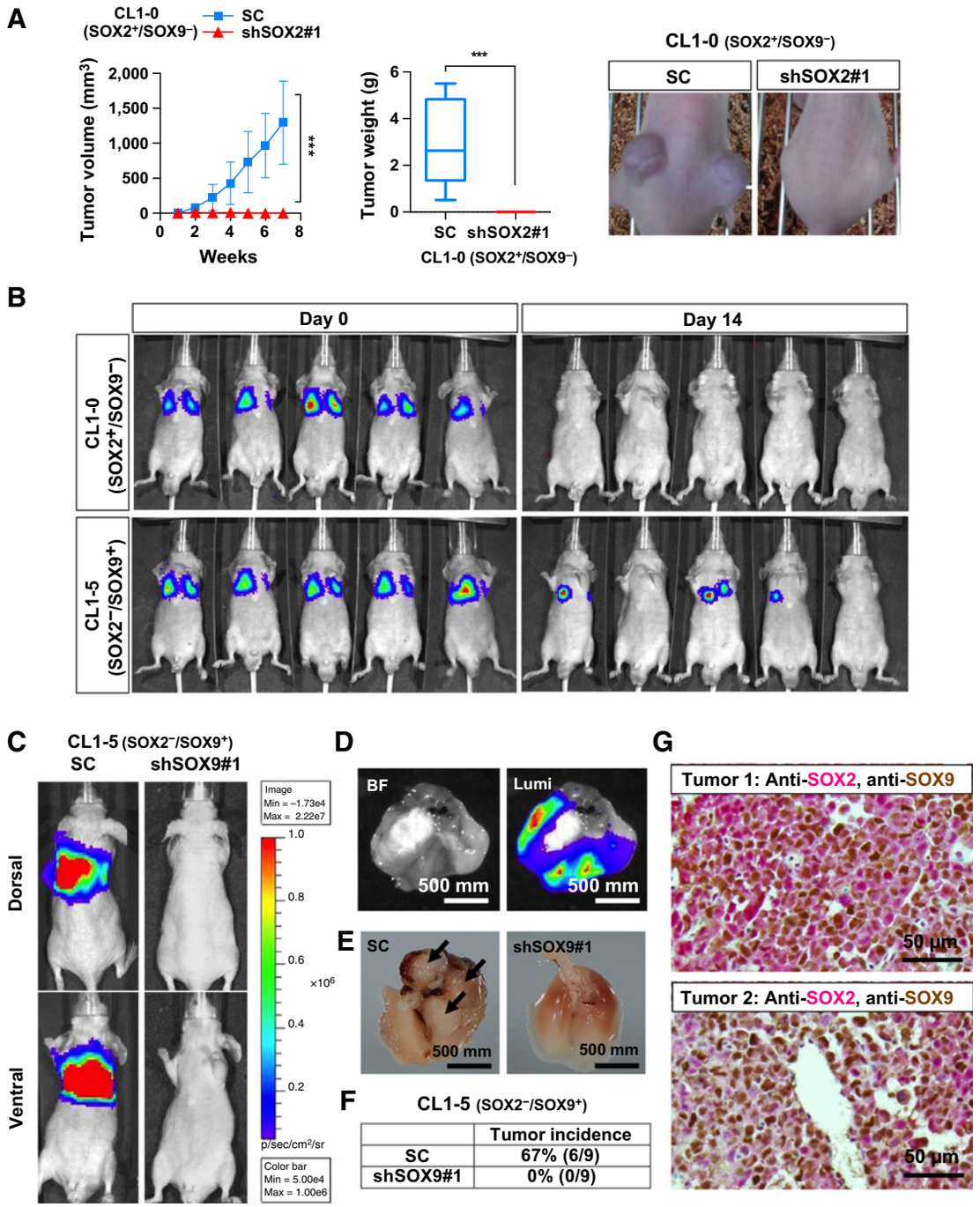

Figure 5.

Roles of SOX2- and SOX9-mediated oncogenesis *in vivo*. **A,** Tumor growth assay of SOX2-silenced lung cancer cells. CL1-0 cells were infected with shSOX2 or scrambled control (SC) lentiviral vectors, followed by subcutaneous xenografted implantation into the flank region of nude mice. Tumor volumes were monitored over time (left). Tumor weights were measured after sacrificing the mice (middle). Bright view of tumor bearing mouse (right). Error bars, SEM ($n = 10$ or $n = 5$). ***, $P < 0.001$. **B,** Bioluminescent images of nude mice intravenously implanted with CL1-0 or CL1-5 cells. **C,** Bioluminescent images of nude mice intravenously implanted with SOX9-silenced CL1-5 cells (right) versus those implanted with the scrambled control cells (left). **D,** Representative bioluminescent signaling in lung tumors derived from CL1-5 cells infected with the scrambled control lentiviral vector. BF, bright field; Lumi, luminescent image. **E,** Bright view of the lung carrying tumors from control CL1-5 cells versus that from SOX9-silenced one. Arrows, tumor nodules. **F,** Lung tumor incidence in mice from control CL1-5 cells versus that from SOX9-silenced one. **G,** Double-staining immunohistochemical analysis of the expression of SOX2 (pink) and SOX9 (brown) in lung tumors derived from scrambled control CL1-5 cells.

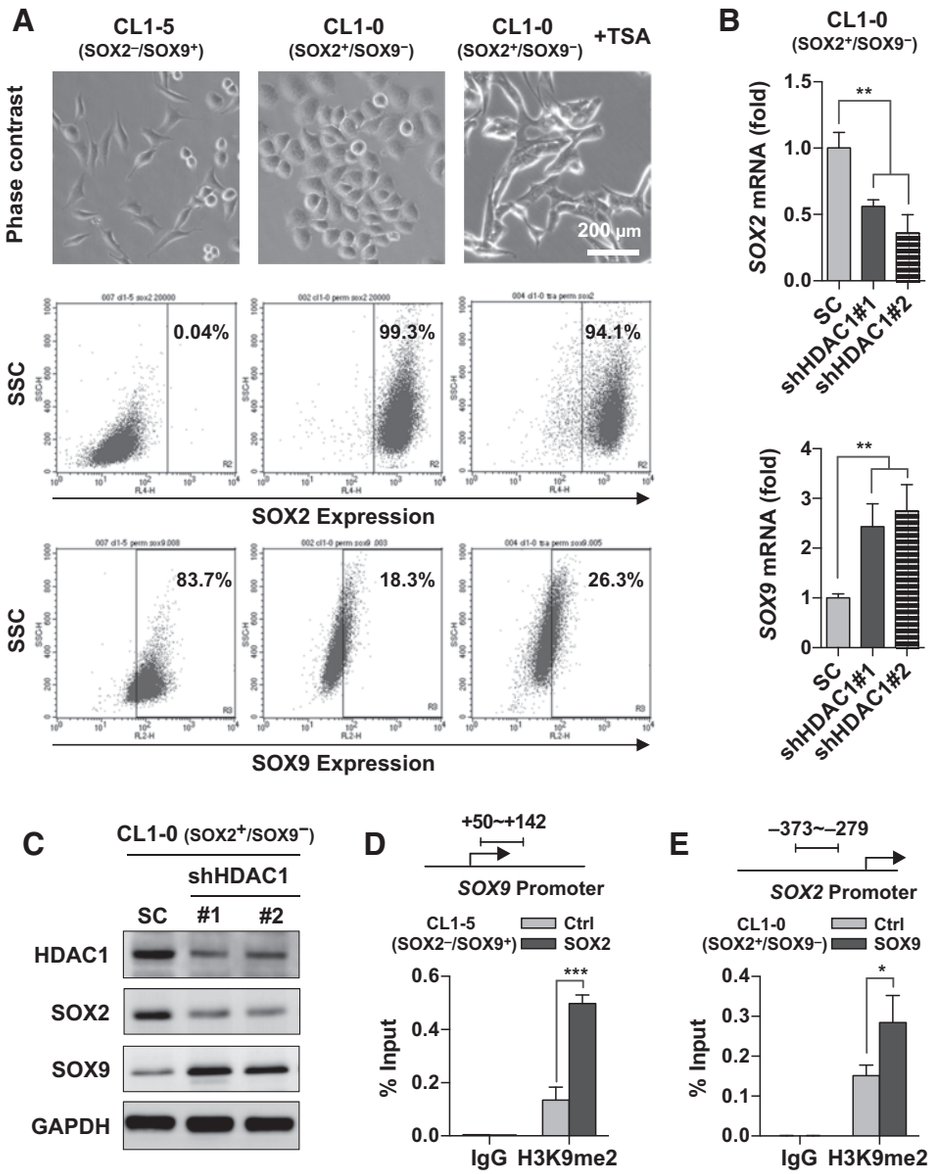

Figure 6.
Epigenetic regulation in *SOX2* and *SOX9* switching. **A,** Phase-contrast images (top) and flow cytometric analysis of CL1-5, CL1-0, and CL1-0 cells treated with TSA (500 nmol/L) to measure SOX2-positve or SOX9-positive populations (middle and bottom, respectively). *x*-axis, SOX2 or SOX9 expression; *y*-axis: SSC. **B,** qPCR analysis for measuring *SOX2* (top) or *SOX9* (bottom) levels in HDAC1-silenced CL1-0 cells. **C,** Western blotting for detecting HDAC1, SOX2, and SOX9 expression in HDAC1-silenced CL1-0 cells. **D,** ChIP assay for comparing H3K9me2 levels on *SOX9* promoter in SOX2-overexpressing CL1-5 and control cells. ***, $P < 0.001$. **E,** ChIP assay for comparing H3K9me2 level on *SOX2* promoter in SOX9-overexpressing CL1-0 with that in control cells. *, $P < 0.05$.

further detected both $SOX2^-/SOX9^+$ and $SOX2^+/SOX9^-$ cells in metastasized lung tumors that had originated from CL1-5 ($SOX2^-/SOX9^+$) cells, which suggests that SOX2 and SOX9 switching might generate heterogeneity in metastatic tumors (Fig. 5G).

Epigenetic modification regulates the SOX2 and SOX9 switch

Because epigenetic regulation contributes to stem/progenitor cell differentiation, CL1-0 cells were treated with trichostatin A (TSA), a histone deacetylase (HDAC) inhibitor, and analyzed via flow cytometry to monitor changes in the SOX2- and SOX9-positive populations and thus assess the involvement of epigenetic regulation in switching between SOX2 and SOX9 expression. Flow cytometric analysis revealed that SOX2-negative cells were rare among untreated CL1-0 cells; however, TSA-mediated pharmacological HDAC inhibition reduced the percentage of SOX2-positive cells while increasing the percentage of SOX9-positive cells, which exhibited a more spindle-like morphology (Fig. 6A). Because SOX2 recruits HDAC1, which in turn regulates SOX2 function (35, 36), we further examined the effects of HDAC1 on the differential expression of SOX2 and SOX9. HDAC1 silencing attenuated the expression of SOX2 but promoted the expression of SOX9, thus suggesting that epigenetic regulation plays a role in switching between SOX2 and SOX9 expression (Fig. 6B and C).

To further examine the involvement of histone modification in the switch between SOX2 and SOX9 expression, a ChIP analysis was conducted to measure the enrichment of dimethylated histone H3 lysine 9 (H3K9me2) on the *SOX9* and *SOX2* promoters upon the expression of SOX2 or SOX9. We found that ectopic SOX2 expression led to elevated H3K9me2 levels on the *SOX9* promoter in CL1-5 cells, thus attenuating the expression of SOX9 (Fig. 6D and Supplementary Figs. S4 and S8). In contrast, SOX9 expression increased the level of H3K9me2 on the *SOX2* promoter in CL1-0 cells (Fig. 6E). Together, our data demonstrate a role for epigenetic regulation in the mutual inhibition between SOX2 and SOX9.

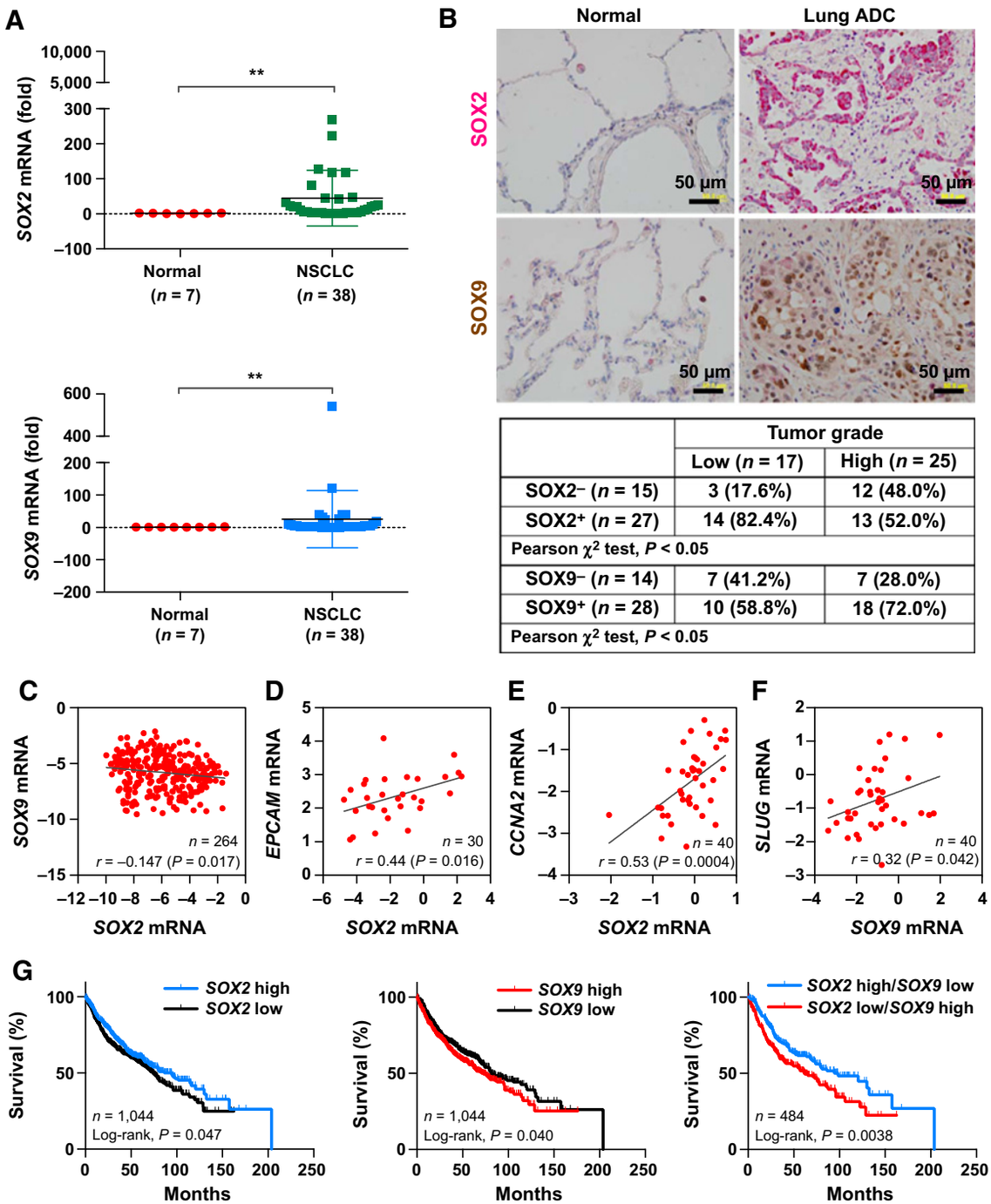

	Tumor grade	
	Low (*n* = 17)	High (*n* = 25)
SOX2⁻ (*n* = 15)	3 (17.6%)	12 (48.0%)
SOX2⁺ (*n* = 27)	14 (82.4%)	13 (52.0%)
Pearson χ^2 test, $P < 0.05$		
SOX9⁻ (*n* = 14)	7 (41.2%)	7 (28.0%)
SOX9⁺ (*n* = 28)	10 (58.8%)	18 (72.0%)
Pearson χ^2 test, $P < 0.05$		

Figure 7.

Correlation analysis of SOX2 and SOX9 levels in primary lung tumors. **A,** qPCR analysis comparing *SOX2* and *SOX9* levels in lung tumors from patients with NSCLC versus nontumor tissues. **B,** Representative immunohistochemical analysis for the expression of SOX2 (pink) and SOX9 (brown) in lung adenocarcinoma versus nontumor tissues (top). Correlation analysis of the expression of SOX2 and SOX9 with tumor grade (bottom). **, $P < 0.01$. Pearson χ^2 correlation analysis of the expression of SOX2 and SOX9 with tumor grade. **C,** A scatter plot generated from primary lung adenocarcinoma (GSE30219) displaying a negative correlation between *SOX2* and *SOX9* levels. **D,** A scatter plot generated from primary lung adenocarcinoma (TCGA) displaying a positive correlation between *SOX2* and *EPCAM* levels. **E,** A scatter plot generated from primary lung adenocarcinoma (GSE3398) displaying a positive correlation between *SOX2* and *CCNA2* levels. **F,** A scatter plot generated from primary lung adenocarcinoma (GSE3398) displaying a positive correlation between *SOX9* and *SLUG* levels. **G,** Kaplan–Meier analysis for the correlation of *SOX2* (left) or *SOX9* (middle) expression with the overall survival of patients with NSCLC ($n = 1{,}044$) from the six databases (GSE4573, GSE14814, GSE3141, GSE19188, GSE31210, and NCI Director's Challenge Consortium). The overall survival data were further stratified by *SOX2* low/*SOX9* high and *SOX2* high/*SOX9* low signatures for Kaplan–Meier analysis (right). Comparative analysis by log-rank test was performed between the different groups.

SOX2 and SOX9 expression correlate with tumor grade in patients with non–small cell lung cancer

The aforementioned results suggest that SOX2 and SOX9 exhibit different oncogenic properties. We next examined *SOX2* and *SOX9* levels in non–small cell lung cancer (NSCLC) tumors and nontumorous tissues. qPCR revealed higher levels of both *SOX2* and *SOX9* in lung tumors, compared with nontumorous tissues (Fig. 7A). Consistent with that finding, an immunohistochemical analysis indicated high levels of both SOX2 and SOX9 in NSCLC tissues (Fig. 7B, top). A correlation analysis revealed that the SOX2 and SOX9 levels were associated with low and high tumor grades, respectively (Fig. 7B, bottom). We further validated this correlation between *SOX2* and *SOX9* levels in primary lung adenocarcinoma. Here, *SOX2* and *SOX9* levels exhibited a negative correlation (Fig. 7C and Supplementary Fig. S9A). Consistent with our *in vitro* analysis, *SOX2* expression was positively associated with *EPCAM* and *CCNA2* expression (Fig. 7D and E and Supplementary Fig. S9B). In contrast, *SOX9* expression correlated with *SLUG* levels in primary lung tumors (Fig. 7F). These findings support the presence of a mutually exclusive pattern of SOX2 and SOX9 expression, leading to the regulation of distinct oncogenic signaling pathways in lung tumors. A Kaplan–Meier survival analysis of patients with NSCLC was conducted to determine the prognostic significance of *SOX2* and *SOX9* expression. We found that a high *SOX2* level correlated with good survival, whereas a high *SOX9* level correlated with poor survival (Fig. 7G, left and middle). Moreover, tumors harboring a *SOX2* low/*SOX9* high signature were associated with worse survival, compared with those carrying a *SOX2* high/*SOX9* low signature (Fig. 7G, right). These data indicate that *SOX2* and *SOX9* might function as prognostic biomarkers in NSCLC.

Discussion

It has long been observed that highly motile cancer cells tend to have lower proliferation rates and vice versa (37–39). In this study, we demonstrated that SOX2 promotes proliferation but inhibits the expression of SOX9, thus maintaining barrier properties. In contrast, SOX9 expression suppresses barrier properties but encourages EMT and invasiveness in lung cancer cells. Our findings support the notion that the switch between SOX2 and SOX9 expression is under epigenetic control and provide critical insights into cancer cell plasticity, which is marked by differential proliferation and invasion abilities of cancer cells.

The intriguing observation that cancer cells exhibit biologic features similar to those of stem/progenitor cells suggests that cancer and stem/progenitor cells share regulatory signaling mechanisms. SOX2 regulates embryonic stem (ES) cell self-renewal and participates in the proliferation of lung progenitor cells, which replenish damaged tissues during bronchiolar injury repair. We found that SOX2 enhances the expression of EpCAM, which inhibits $p21^{Cip1}$ but induces cyclin A2 and thus promotes increased lung cancer cell proliferation. SOX2 has consistently been found to regulate cancer stem cells and thus encourage tumor initiation in lung and other types of cancer (10, 19). SOX2 or EpCAM is reported to promote cisplatin chemoresistance via enhanced survival signaling in lung and other cancer cells (10, 40). Here, we observed that SOX2-positive cells are more resistant to cisplatin than are SOX9-positive cells (Fig. 1E and Supplementary Fig. S1). In mice, Sox2 regulates squamous skin tumor cell proliferation and stemness features via direct and/or indirect control of downstream targets, such as *Ccnd2*, *Cdkn2a*, and *Trp63* (10, 19). Moreover, SOX2 interacts with CTNNB1 to activate cyclin D1–dependent proliferation in breast cancer cells (15, 16), suggesting that SOX2 promotes tumor growth by regulating distinct downstream targets in different cells. In addition, EpCAM promotes the reprogramming of fibroblasts into iPS cells, whereas $p21^{Cip1}$ inhibits this process (41, 42). Our data suggest that the SOX2–EpCAM–$p21^{Cip1}$–cyclin A2 pathway not only elicits stem/progenitor cell–like features but also encourages malignancy.

In contrast to SOX2, SOX9 expression accelerates ES cell differentiation via a $p21^{Cip1}$-dependent pathway and contributes to chondrogenesis (43). We observed that SOX9 expression induces mesenchymal morphology, whereas SOX9 silencing induces barrier properties, suggesting a critical role for SOX9 in EMT in lung cancer cells. SLUG, a key regulator of EMT, is overexpressed and thus encourages invasion in a subgroup of lung cancer (44). We found that SOX9 binds the *SLUG* promoter to induce its expression. Sox9–Slug signaling was previously reported to regulate avian neural crest development (20) and to enhance metastatic potential in a mouse tumor model (23). Consistently, we observed that SOX9 silencing attenuated SLUG expression and inhibited lung cancer cell invasion *in vitro* and in animal models. Moreover, we found that in lung tumors, SOX9 expression correlated with an advanced tumor grade and *SLUG* levels. Our findings support the involvement of SOX9–SLUG signaling in lung cancer cell invasion.

Although EMT has been attributed to cancer dissemination, several reports indicate that MET, a reversal of EMT, is critical for cancer metastasis (3–5), particularly with regard to cancer cell seeding and colonization in distant organs. In addition, increased barrier properties, mediated by adhesion molecules, such as EpCAM and E-cadherin, have been suggested to support cell proliferation and survival. Although our data suggest that the SOX2–EpCAM–$p21^{Cip1}$–cyclin A2 pathway inhibits cancer cell invasion, we observed the presence of both $SOX2^-/SOX9^+$ and $SOX2^+/SOX9^-$ cells in metastases of intravenously injected lung tumors (Fig. 5G). The involvement of SOX2-mediated MET in cancer metastasis requires further investigation.

By selecting invasive lung cancer cells from noninvasive $SOX2^+/SOX9^-$ lung cancer cells, we discovered that SOX9 programming switched on while SOX2 program switched off. Upon enriching the endogenous expression of SOX2 in $SOX2^-/SOX9^+$ invasive lung cancer cells, we observed that the SOX9 program was turned off, accompanied by increased proliferative but decreased invasive abilities. Epigenetic regulation mediates stem/progenitor cell differentiation and iPS cell reprogramming, a process that can be further boosted by HDAC inhibitors (45, 46). By using TSA to inhibit HDACs in $SOX2^+/SOX9^-$ cells followed by flow cytometry to analyze SOX2 and SOX9 expression, we observed an increase in the $SOX2^-/SOX9^+$ population. Moreover, ectopic SOX2 expression in $SOX2^-/SOX9^+$ lung cancer cells led to elevated H3K9me2 levels on the *SOX9* promoter and attenuated SOX9 expression and vice versa. In agreement with these findings, we observed the reciprocal enrichment of H3K9me2 on the *SOX2* and *SOX9* promoters of CL1-1 and CL1-2 cells (Supplementary Fig. S8), which exhibit distinct phenotypic features and oncogenic properties as described in Fig. 1. Although SOX2 interacts with HDAC1, the functional role of this interaction had not previously been addressed. We observed that HDAC1 silencing increased SOX9 expression, further demonstrating the involvement of HDAC1 in the switch between SOX2 and SOX9 expression. A

correlation analysis of lung adenocarcinoma cohorts indicated a positive association between *SOX2* and *HDAC1* levels (Supplementary Fig. S9C). Our findings support the critical involvement of epigenetic regulation in the switch between SOX2 and SOX9 expression. Although the observation that epigenetic regulation between *SOX2* and *SOX9* creates cancer plasticity with the switch between epithelial-like and mesenchymal-like states may imply stem cell differentiation and dedifferentiation, we do not have direct evidence for the involvement of cancer stem cells in these phenomena.

Taken together, our data indicate that a subgroup of lung cancer cells adopts SOX2–EpCAM–$p21^{Cip1}$–cyclin A2 signaling to promote cell proliferation. In contrast, SOX9–SLUG signaling induces EMT and promotes cancer cell invasion. Cancer cell plasticity, indicated by a switch between SOX2 and SOX9 expression programs, is under epigenetic control and endows cancer cells with different proliferative and invasive abilities, as well as the morphological plasticity to cope with selection pressures (Supplementary Fig. S10). These findings provide new insights into the role of epigenetic-mediated cancer cell plasticity in tumor progression.

Disclosure of Potential Conflicts of Interest

No potential conflicts of interest were disclosed.

Authors' Contributions

Conception and design: Y.-T. Chou, S.S. Jiang

Development of methodology: Y.-T. Chou, J.-L. Chang

Acquisition of data (provided animals, acquired and managed patients, provided facilities, etc.): S.-C. Lin, Y.-T. Chou, J.-L. Chang, Y.-R. Kao

Analysis and interpretation of data (e.g., statistical analysis, biostatistics, computational analysis): S.-C. Lin, Y.-T. Chou, S.S. Jiang, J.-L. Chang, C.-H. Chung, Y.-R. Kao, I-S. Chang

Writing, review, and/or revision of the manuscript: S.-C. Lin, Y.-T. Chou, C.-W. Wu

Administrative, technical, or material support (i.e., reporting or organizing data, constructing databases): Y.-T. Chou, J.-L. Chang, Y.-R. Kao, C.-W. Wu

Study supervision: Y.-T. Chou, C.-W. Wu

Acknowledgments

Sheng-Chieh Lin carried out his thesis research under the auspices of the Graduate Program of Biotechnology in Medicine, National Tsing Hua University, and National Health Research Institutes.

Grant Support

This work was supported by the Institute of Biomedical Science at Academia Sinica, National Yang-Ming University, National Tsing Hua University, and Ministry of Science and Technology (MOST104-2321-B-010-007 and MOST103-2320-B-007-006-MY3), Executive Yuan, Taiwan.

The costs of publication of this article were defrayed in part by the payment of page charges. This article must therefore be hereby marked *advertisement* in accordance with 18 U.S.C. Section 1734 solely to indicate this fact.

Received November 22, 2015; revised September 22, 2016; accepted September 25, 2016; published OnlineFirst October 7, 2016.

References

1. Cano A, Perez-Moreno MA, Rodrigo I, Locascio A, Blanco MJ, del Barrio MG, et al. The transcription factor snail controls epithelial-mesenchymal transitions by repressing E-cadherin expression. Nat Cell Biol 2000;2:76–83.
2. Boyer B, Thiery JP. Epithelium-mesenchyme interconversion as example of epithelial plasticity. APMIS 1993;101:257–68.
3. Ocana OH, Corcoles R, Fabra A, Moreno-Bueno G, Acloque H, Vega S, et al. Metastatic colonization requires the repression of the epithelial-mesenchymal transition inducer Prrx1. Cancer Cell 2012;22:709–24.
4. Tsai JH, Donaher JL, Murphy DA, Chau S, Yang J. Spatiotemporal regulation of epithelial-mesenchymal transition is essential for squamous cell carcinoma metastasis. Cancer Cell 2012;22:725–36.
5. Chaffer CL, Brennan JP, Slavin JL, Blick T, Thompson EW, Williams ED. Mesenchymal-to-epithelial transition facilitates bladder cancer metastasis: role of fibroblast growth factor receptor-2. Cancer Res 2006;66:11271–8.
6. Liu S, Cong Y, Wang D, Sun Y, Deng L, Liu Y, et al. Breast cancer stem cells transition between epithelial and mesenchymal states reflective of their normal counterparts. Stem Cell Rep 2014;2:78–91.
7. Shipitsin M, Campbell LL, Argani P, Weremowicz S, Bloushtain-Qimron N, Yao J, et al. Molecular definition of breast tumor heterogeneity. Cancer Cell 2007;11:259–73.
8. Hnisz D, Abraham BJ, Lee TI, Lau A, Saint-Andre V, Sigova AA, et al. Super-enhancers in the control of cell identity and disease. Cell 2013;155:934–47.
9. Adam RC, Yang H, Rockowitz S, Larsen SB, Nikolova M, Oristian DS, et al. Pioneer factors govern super-enhancer dynamics in stem cell plasticity and lineage choice. Nature 2015;521:366–70.
10. Chou YT, Lee CC, Hsiao SH, Lin SE, Lin SC, Chung CH, et al. The emerging role of SOX2 in cell proliferation and survival and its crosstalk with oncogenic signaling in lung cancer. Stem Cells 2013;31:2607–19.
11. Doe CQ. Neural stem cells: balancing self-renewal with differentiation. Development 2008;135:1575–87.
12. Chen X, Vega VB, Ng HH. Transcriptional regulatory networks in embryonic stem cells. Cold Spring Harb Symp Quant Biol 2008;73:203–9.
13. Que J, Luo X, Schwartz RJ, Hogan BL. Multiple roles for Sox2 in the developing and adult mouse trachea. Development 2009;136:1899–907.
14. Tompkins DH, Besnard V, Lange AW, Wert SE, Keiser AR, Smith AN, et al. Sox2 is required for maintenance and differentiation of bronchiolar Clara, ciliated, and goblet cells. PLoS One 2009;4:e8248.
15. Chen Y, Shi L, Zhang L, Li R, Liang J, Yu W, et al. The molecular mechanism governing the oncogenic potential of SOX2 in breast cancer. J Biol Chem 2008;283:17969–78.
16. Sholl LM, Long KB, Hornick JL. Sox2 expression in pulmonary non-small cell and neuroendocrine carcinomas. Appl Immunohistochem Mol Morphol 2010;18:55–61.
17. Bass AJ, Watanabe H, Mermel CH, Yu S, Perner S, Verhaak RG, et al. SOX2 is an amplified lineage-survival oncogene in lung and esophageal squamous cell carcinomas. Nat Genet 2009;41:1238–42.
18. Lu Y, Futtner C, Rock JR, Xu X, Whitworth W, Hogan BL, et al. Evidence that SOX2 overexpression is oncogenic in the lung. PLoS One 2010;5:e11022.
19. Boumahdi S, Driessens G, Lapouge G, Rorive S, Nassar D, Le Mercier M, et al. SOX2 controls tumour initiation and cancer stem-cell functions in squamous-cell carcinoma. Nature 2014;511:246–50.
20. Sakai D, Suzuki T, Osumi N, Wakamatsu Y. Cooperative action of Sox9, Snail2 and PKA signaling in early neural crest development. Development 2006;133:1323–33.
21. Rockich BE, Hrycaj SM, Shih HP, Nagy MS, Ferguson MA, Kopp JL, et al. Sox9 plays multiple roles in the lung epithelium during branching morphogenesis. Proc Natl Acad Sci U S A 2013;110:E4456–64.
22. Jiang SS, Fang WT, Hou YH, Huang SF, Yen BL, Chang JL, et al. Upregulation of SOX9 in lung adenocarcinoma and its involvement in the regulation of cell growth and tumorigenicity. Clin Cancer Res 2010;16:4363–73.
23. Guo W, Keckesova Z, Donaher JL, Shibue T, Tischler V, Reinhardt F, et al. Slug and Sox9 cooperatively determine the mammary stem cell state. Cell 2012;148:1015–28.
24. Akiyama H, Chaboissier MC, Martin JF, Schedl A, de Crombrugghe B. The transcription factor Sox9 has essential roles in successive steps of the chondrocyte differentiation pathway and is required for expression of Sox5 and Sox6. Genes Dev 2002;16:2813–28.
25. Chu YW, Yang PC, Yang SC, Shyu YC, Hendrix MJ, Wu R, et al. Selection of invasive and metastatic subpopulations from a human lung adenocarcinoma cell line. Am J Respir Cell Mol Biol 1997;17:353–60.

26. Chou YT, Hsieh CH, Chiou SH, Hsu CF, Kao YR, Lee CC, et al. CITED2 functions as a molecular switch of cytokine-induced proliferation and quiescence. Cell Death Differ 2012;19:2015–28.
27. Chou YT, Lin HH, Lien YC, Wang YH, Hong CF, Kao YR, et al. EGFR promotes lung tumorigenesis by activating miR-7 through a Ras/ERK/Myc pathway that targets the Ets2 transcriptional repressor ERF. Cancer Res 2010;70:8822–31.
28. Hotta A, Cheung AY, Farra N, Vijayaragavan K, Seguin CA, Draper JS, et al. Isolation of human iPS cells using EOS lentiviral vectors to select for pluripotency. Nat Methods 2009;6:370–6.
29. Osta WA, Chen Y, Mikhitarian K, Mitas M, Salem M, Hannun YA, et al. EpCAM is overexpressed in breast cancer and is a potential target for breast cancer gene therapy. Cancer Res 2004;64:5818–24.
30. Gonzalez B, Denzel S, Mack B, Conrad M, Gires O. EpCAM is involved in maintenance of the murine embryonic stem cell phenotype. Stem Cells 2009;27:1782–91.
31. Ng VY, Ang SN, Chan JX, Choo AB. Characterization of epithelial cell adhesion molecule as a surface marker on undifferentiated human embryonic stem cells. Stem Cells 2010;28:29–35.
32. Shen CI, Lee HC, Kao YH, Wu CS, Chen PH, Lin SZ, et al. EpCAM induction functionally links to the Wnt-enhanced cell proliferation in human keratinocytes. Cell Transplant 2014;23:1031–44.
33. Chao Y, Shih YL, Chiu JH, Chau GY, Lui WY, Yang WK, et al. Overexpression of cyclin A but not Skp 2 correlates with the tumor relapse of human hepatocellular carcinoma. Cancer Res 1998;58:985–90.
34. Chen HM, Yen-Ping Kuo M, Lin KH, Lin CY, Chiang CP. Expression of cyclin A is related to progression of oral squamous cell carcinoma in Taiwan. Oral Oncol 2003;39:476–82.
35. Cox JL, Mallanna SK, Luo X, Rizzino A. Sox2 uses multiple domains to associate with proteins present in Sox2-protein complexes. PLoS One 2010;5:e15486.
36. Kidder BL, Palmer S. HDAC1 regulates pluripotency and lineage specific transcriptional networks in embryonic and trophoblast stem cells. Nucleic Acids Res 2012;40:2925–39.
37. Giese A, Loo MA, Tran N, Haskett D, Coons SW, Berens ME. Dichotomy of astrocytoma migration and proliferation. Int J Cancer 1996;67:275–82.
38. Shiwarski DJ, Shao C, Bill A, Kim J, Xiao D, Bertrand CA, et al. To "grow" or "go": TMEM16A expression as a switch between tumor growth and metastasis in SCCHN. Clin Cancer Res 2014;20:4673–88.
39. Giese A, Bjerkvig R, Berens ME, Westphal M. Cost of migration: invasion of malignant gliomas and implications for treatment. J Clin Oncol 2003;21:1624–36.
40. Kimura O, Kondo Y, Kogure T, Kakazu E, Ninomiya M, Iwata T, et al. Expression of EpCAM increases in the hepatitis B related and the treatment-resistant hepatocellular carcinoma. Biomed Res Int 2014;2014:172913.
41. Huang HP, Chen PH, Yu CY, Chuang CY, Stone L, Hsiao WC, et al. Epithelial cell adhesion molecule (EpCAM) complex proteins promote transcription factor-mediated pluripotency reprogramming. J Biol Chem 2011;286:33520–32.
42. Hong H, Takahashi K, Ichisaka T, Aoi T, Kanagawa O, Nakagawa M, et al. Suppression of induced pluripotent stem cell generation by the p53-p21 pathway. Nature 2009;460:1132–5.
43. Yamamizu K, Schlessinger D, Ko MS. SOX9 accelerates ESC differentiation to three germ layer lineages by repressing SOX2 expression through P21 (WAF1/CIP1). Development 2014;141:4254–66.
44. Shih JY, Tsai MF, Chang TH, Chang YL, Yuan A, Yu CJ, et al. Transcription repressor slug promotes carcinoma invasion and predicts outcome of patients with lung adenocarcinoma. Clin Cancer Res 2005;11:8070–8.
45. Huangfu D, Maehr R, Guo W, Eijkelenboom A, Snitow M, Chen AE, et al. Induction of pluripotent stem cells by defined factors is greatly improved by small-molecule compounds. Nat Biotechnol 2008;26:795–7.
46. Lim SY, Sivakumaran P, Crombie DE, Dusting GJ, Pebay A, Dilley RJ. Trichostatin A enhances differentiation of human induced pluripotent stem cells to cardiogenic cells for cardiac tissue engineering. Stem Cells Transl Med 2013;2:715–25.